Supramolecular interactions induced hinge-like motion of a metal-organic framework accompanied by anisotropic thermal expansion

Lei Zhang, Xiaofei Kuang, Xiaoyuan Wu, Wenbin Yang and Canzhong Lu*

Experimental Section

General procedure All solvents and reagents were purchased from commercial sources and used without purification. Elemental analyses of (C, H and N) were carried out with a Vario EL III elemental analyzer. Thermogravimetric analysis (TGA) and Mass spectrometer (MS) performed with a STA449C-QMS 403 C at a heating rate of 5 ºC/min under nitrogen atmosphere. Differential Scanning CaLorimetry (DSC) data was measured by NETZSCH DTA 404PC. Powder X-ray diffraction (PXRD) was performed with a Rigaku DMAX 2500 diffractometer using Cu *K*α radiation (λ = 0.154 nm). Fluorescence spectra were recorded on a HORIBA Jobin-Yvon FluoroMax-4 spectrometer. Optical diffuse reflectance spectra were measured on a PE Lambda 900 UV-Vis spectrophotometer. Variable temperature powder X-ray diffraction (VT-PXRD) data were collected X'Pert PRO.

Synthesis procedure

Tris-(4-pyridyl)-1,3,5-triazine (tpt) was synthesized according to a literature method.[1]

Synthesis of $Ag_4(tpt)_4[Mo_8O_{26}]\cdot 1.5H_2O$ (A) $(NH_4)_6Mo_7O_{24}\cdot 4H_2O$ (0.1125 g, 0.091 mmol) and CH_3COOAg (0.0536 g, 0.321 mmol) were stirred for 0.5 h in 10 ml distilled water at room temperature, then tpt (0.0603 g, 1.933 mmol) was added and stirred for 2 h. The pH value of the solution was adjusted to *ca*. 4.35 by 2M HCl, and then the suspension was placed in a 20 ml Teflon-lined autoclave and kept under autogenous pressure at 180 ºC for 6 days. After slow cooling to room temperature for another 6 days, pale yellow crystals of **A** were filtered and washed with distilled water. (Yield: 29.6% based on silver). Anal. Calcd (Found %) for $C_{72}H_{51}Ag_4Mo_8N_{24}O_{27}$ **A**: C, 29.99 (29.97); H, 1.78(1.99); N, 11.66 (11.62).

The dehydrated phase $Ag_4(tpt)_4[Mo_8O_{26}]$ (B) The dehydrated phase **B** was obtained by heating **A** at 100 ºC for several hours**.** Anal. Calcd (Found %) for $C_{72}H_{48}Ag_4Mo_8N_{24}O_{26}$ **B**: C, 30.19 (29.89); H, 1.69(1.88); N, 11.74 (11.78).

Crystallographic study

According to the literature that in situ X-ray diffraction studies on single crystals relate to framework flexibilities on removal of solvent can give important information about the thermally induced structural changes in MOFs.[2] Therefore, we determine the thermal expansion behaviors for **A** and the dehydrated phase **B** using single crystal X-ray diffraction. Variable-temperature single-crystal X-ray diffraction experiments were carried out on an Oxford Diffraction/Agilent SuperNova diffractometer (graphite-monochromated Mo K_α radiation, λ= 0.71073 Å) fitted with an Oxford Cryosystems Cryostream 700 open flow cooling device.[3] The CrystalClear program was used for the absorption correction. The structure was solved by direct methods and refined on F^2 by full-matrix, least-squares methods using the SHELXL-97 program package.[4] All non-hydrogen atoms were refined anisotropically. The hydrogen atoms for the tpt ligands were placed in calculated positions and treated as riding on their parents. The crystals were supported on top of a glass fiber and mounted in the open nitrogen flow from a nitrogen cryostream (Oxford). A full set of reflections were collected in the temperature range 100-500 K with 30 K intervals and after holding at 15 min at each temperature. A summary of crystallographic refinement details is given in table S1 for **A** at 100 K and **B** at 100 K. Unit cell parameters, the Ag···Ag distance and centroid–centroid distance between triazine rings and pyridyl rings of head-to-tail conformation, as well as the length of hydrogen bonds as a function of temperature for **A** at ambient pressure in table S2, moreover, unit cell parameters, the Ag···Ag distance and centroid–centroid distance between triazine rings and pyridyl rings of head-to-tail conformation as a function of temperature for **B** at ambient pressure in table S3. In consideration of the reversibility of the phenomenon which is very important in case of thermal expans ion, when the test temperature of **A** is up to 500 K (**A** has converted to the dehydrated phase **B** and its cooling form as **A'**), then it slowly returns to 160 K in table S4. Complete details can be found in the accompanying cif file. The CCDC (956831-956845) is for **A-warming** (100-500 K), CCDC (976108-976113) is for **A'-cooling** (440-160 K) and CCDC (956846-956860) is for **B-warming** (100-500 K).

Table S1 A summary of crystallographic refinement details is given in Tables S1 for **A** at 100 K, and **B** at 100 K.

	A	**B**
Empirical formula	C72H51Ag4Mo8N24O27.50	C72H48Ag4Mo8N24O26
Formula weight	2891.37	2864.34
Temperature	100 K	100 K
Wavelength	0.71073 Å	0.71073 Å
Space group	C2/c	C2/c
Unit cell dimensions	a = 22.0765 (5) Å α = 90°	a = 22.1162 (7) Å α = 90°
	b = 16.3158 (5) Å β = 115.416 (4)°	b = 16.2831(4) Å β = 115.366 (4)°
	c = 25.6800 (8) Å γ = 90°	c = 25.6433 (12) Å γ = 90°
Volume	8354.6 (4)	8344.4(5)
Z	4	4
Density (calculated)	2.299 g/cm^3	2.280 g/cm^3
Absorption coefficient	2.167 mm^{-1}	2.167 mm^{-1}
F (000)	5580.0	5520.0
Crystal size	0.30× 0.15 × 0.10 mm	0.30× 0.15× 0.10 mm
Theta range for data collection	3.07° to 25°	3.06° to 25°
Index ranges	-21 <= h <= 26	-26 <= h <= 26
	-18 <= k <= 19	-19 <= k <= 19
	-30 <= l <= 20	-30 <= l <= 25
Reflections collected	19300	13579
Independent reflections	7157 [R(int) = 0.0300]	6719 [R(int) = 0.0383]
Absorption correction	Multi-scan	Multi-scan
Refinement method	Full-matrix least-squares on F^2	Full-matrix least-squares on F^2
Data / restraints / parameters	7157 / 0 / 616	6719 / 0 / 605
Goodness-of-fit on F^2	1.043	1.059
Final R indices [I>2sigma(I)]	$R_1 = 0.0300$	$R_1 = 0.0383$
	$wR_2 = 0.0732$	$wR_2 = 0.1064$
R indices (all data)	$R_1 = 0.0340$	$R_1 = 0.0440$
	$wR_2 = 0.0758$	$wR_2 = 0.1110$
Largest diff. peak and hole	1.709 and -1.843 e·Å^{-3}	2.809 and -2.278 e·Å^{-3}

Table S2 Variable-temperature lattice parameter data, the Ag⋯Ag distance and centroid–centroid distance between triazine rings and pyridyl rings of head-to-tail conformation, as well as the length of hydrogen bond for **A** as determined using single crystal X-ray diffraction upon warming from 100 K to 500 K.[a]

T (K)	a (Å)	b (Å)	c (Å)	α (°)	β (°)	γ (°)	V (Å)
100.01 (15)	22.0765 (5)	16.3158 (5)	25.6800 (8)	90	115.416 (4)	90	8354.6 (4)
130.01 (10)	22.0600 (5)	16.3472 (5)	25.6770 (8)	90	115.392 (4)	90	8365.1 (4)
160.01 (10)	22.0532 (5)	16.3828 (5)	25.6809 (8)	90	115.391 (4)	90	8382.1 (4)
190.01 (10)	22.0383 (6)	16.4151 (6)	25.6790 (8)	90	115.404 (4)	90	8391.4 (4)
220.00 (10)	22.0366 (6)	16.4532 (6)	25.6805 (8)	90	115.397 (4)	90	8411.2 (5)
250.01 (10)	22.0248 (6)	16.4933 (6)	25.6766 (8)	90	115.385 (4)	90	8426.7 (4)
280.00 (10)	22.0121 (6)	16.5301 (6)	25.6641 (9)	90	115.386 (5)	90	8436.5 (5)
310.00 (10)	21.9848 (6)	16.5617 (6)	25.6443 (9)	90	115.366 (5)	90	8437.0 (5)
340.01 (10)	21.9777 (6)	16.6111 (6)	25.6344 (9)	90	115.351 (5)	90	8457.2 (5)
370.00 (10)	21.9944 (8)	16.6621 (5)	25.6363 (11)	90	115.340 (5)	90	8491.1 (5)
380.00 (10)	21.9717 (6)	16.6692 (6)	25.6289 (9)	90	115.344 (5)	90	8483.2 (5)
410.01 (10)	21.9504 (7)	16.7095 (7)	25.6128 (10)	90	115.366 (5)	90	8488.6 (6)
440.01 (10)	21.9362 (7)	16.7329 (5)	25.5715 (11)	90	115.324 (4)	90	8484.2 (5)
470.00 (10)	21.9416 (8)	16.7734 (6)	25.5513 (14)	90	115.225 (5)	90	8507.0 (6)
500.00 (10)	21.9368 (7)	16.8155 (5)	25.4998 (12)	90	115.121 (4)	90	8516.6 (5)

T (K)	Ag⋯Ag (Å)	π-π (Å)	O_{13}…O_{14} (Å)
100.01 (15)	3.4051 (5)	3.5154 (1)	2.8872 (93)
130.01 (10)	3.4221 (5)	3.5218 (1)	2.8801 (90)
160.01 (10)	3.4380 (5)	3.5296 (1)	2.8817 (94)
190.01 (10)	3.4509 (5)	3.5330 (1)	2.8650 (94)
220.00 (10)	3.4656 (5)	3.5405 (1)	2.8611 (103)
250.01 (10)	3.4827 (5)	3.5488 (1)	2.8639 (103)
280.00 (10)	3.4991 (5)	3.5572 (1)	2.8589 (120)
310.00 (10)	3.5144 (7)	3.5641 (1)	2.8632 (137)
340.01 (10)	3.5327 (7)	3.5753 (1)	2.8750 (174)
370.00 (10)	3.5521 (8)	3.5877 (1)	
380.00 (10)	3.5567 (9)	3.5938 (1)	
410.01 (10)	3.5744 (10)	3.6056 (1)	
440.01 (10)	3.5880 (11)	3.6153 (1)	
470.00 (10)	3.6059 (12)	3.6366 (1)	
500.00 (10)	3.6238 (13)	3.6663 (1)	

[a] Compound **A** has lost water at 370 K, **A** has converted to the dehydrated phase **B**. Estimated standard deviations are given in parentheses.

Table S3 Unit cell parameters, the Ag···Ag distance and centroid–centroid distance between triazine rings and pyridyl rings of head-to-tail conformation as a function of temperature for **B.**

T (K)	a (Å)	b (Å)	c (Å)	α (°)	β (°)	γ (°)	V (Å)
100.01 (11)	22.1162 (7)	16.2831 (4)	25.6433 (12)	90	115.366 (4)	90	8344.4 (5)
130.00 (10)	22.0935 (9)	16.2897 (4)	25.6306 (11)	90	115.277 (5)	90	8341.2 (5)
160.01 (10)	22.0870 (8)	16.3172 (4)	25.6279 (10)	90	115.265 (5)	90	8352.7 (5)
190.00 (10)	22.0639 (8)	16.3382 (4)	25.6170 (10)	90	115.311 (4)	90	8348.0 (5)
220.01 (10)	22.0572 (6)	16.3893 (3)	25.6030 (7)	90	115.305 (3)	90	8367.4 (4)
250.01 (10)	22.0466 (6)	16.4250 (3)	25.5931 (7)	90	115.293 (3)	90	8379.2 (4)
310.01 (10)	22.0290 (9)	16.4861 (5)	25.5887 (11)	90	115.233 (5)	90	8406.4 (6)
340.00 (10)	22.0101 (9)	16.5266 (5)	25.5684 (11)	90	115.234 (5)	90	8413.0 (6)
370.01 (10)	21.9943 (8)	16.5773 (6)	25.5580 (15)	90	115.203 (5)	90	8431.5 (7)
380.00 (10)	21.9867 (10)	16.5916 (5)	25.5520 (12)	90	115.203 (6)	90	8433.9 (6)
410.01 (10)	21.9660 (9)	16.6288 (6)	25.5315 (16)	90	115.158 (6)	90	8441.2 (7)
440.00 (10)	21.9475 (9)	16.6741 (7)	25.5226 (17)	90	115.119 (6)	90	8456.8 (8)
470.00 (10)	21.9381 (12)	16.7198 (7)	25.5037 (14)	90	115.074 (7)	90	8473.2 (7)
500.00 (10)	21.9302 (11)	16.7795 (8)	25.4880 (18)	90	115.029 (7)	90	8498.3 (8)

T (K)	Ag···Ag (Å)	π-π (Å)
100.01 (11)	3.4271 (7)	3.5308 (1)
130.00 (10)	3.4338 (7)	3.5286 (1)
160.01 (10)	3.4457 (7)	3.5349 (1)
190.00 (10)	3.4549 (7)	3.5382 (1)
220.01 (10)	3.4718 (7)	3.5476 (1)
250.01 (10)	3.4869 (7)	3.5568 (1)
310.01 (10)	3.5134 (8)	3.5762 (1)
340.00 (10)	3.5296 (9)	3.5874 (1)
370.01 (10)	3.5477 (11)	3.6015 (1)
380.00 (10)	3.5528 (11)	3.6047 (1)
410.01 (10)	3.5668 (12)	3.6124 (1)
440.00 (10)	3.5823 (13)	3.6255 (1)
470.00 (10)	3.5991 (13)	3.6470 (1)
500.00 (10)	3.6194 (14)	3.6649 (2)

Estimated standard deviations are given in parentheses.

Table S4 Variable-temperature lattice parameter data of **A’** (**A** has converted to the dehydrated phase **B**) as determined using single crystal X-ray diffraction upon cooling from 500 K to 160 K.

T (K)	a (Å)	b (Å)	c (Å)	α (°)	β (°)	γ (°)	V(Å)
500.00 (10)	21.9368 (7)	16.8155 (5)	25.4998 (12)	90	115.121 (4)	90	8516.6 (5)
440.00 (10)	22.0200 (8)	16.7356 (6)	25.5607 (14)	90	115.199 (5)	90	8516.2 (6)
370.00 (10)	22.0267 (7)	16.6061 (5)	25.5742 (12)	90	115.250 (4)	90	8460.7 (5)
310.01 (10)	22.0501 (7)	16.5079 (5)	25.5960 (12)	90	115.291 (4)	90	8423.9 (5)
250.01 (10)	22.0700 (7)	16.4328 (4)	25.6173 (12)	90	115.315 (4)	90	8398.5 (5)
210.00 (10)	22.0780 (70	16.3817 (4)	25.6311 (11)	90	115.334 (4)	90	8378.6 (5)
160.01 (10)	22.0984 (6)	16.3321 (4)	25.6479 (11)	90	115.350 (4)	90	8365.3 (5)

Estimated standard deviations are given in parentheses.

Table S5 Principal axis of thermal expansion of **A** determined by PASCal from 100 K to 340 K.[5]

Axes of thermal expansion	**Direction**				
	α(MK^{-1})	**σα(MK^{-1})**	***a***	***b***	***c***
X1	-18.0769	0.9060	-0.9931	0.0000	-0.1177
X2	-5.1208	1.5096	0.3389	-0.0000	0.9408
X3	74.8252	1.4212	0.0000	-1.0000	0.0000
V	52.1460	1.8459			

Table S6 Principal axis of thermal expansion of **B** determined by PASCal from 100 K to 340 K.[5]

Axes of thermal expansion	Direction				
	α(MK^{-1})	**σα(MK^{-1})**	***a***	***b***	***c***
X1	-18.6099	1.2146	-0.9856	0.0000	0.1690
X2	-8.0369	1.5380	0.5567	-0.0000	0.8307
X3	65.4532	3.2996	0.0000	-1.0000	0.0000
V	41.3568	3.5107			

Table S7 Principal axis of thermal expansion of **B** determined by PASCal from 100 K to 500 K.[5]

Axes of thermal expansion	Direction				
	α(MK^{-1})	**σα(MK^{-1})**	***a***	***b***	***c***
X1	-22.3196	0.6765	-0.9720	0.0000	-0.2349
X2	-7.4736	0.7067	-0.5915	-0.0000	0.8063
X3	77.2409	2.9627	0.0000	-1.0000	0.0000
V	47.9789	2.7759			

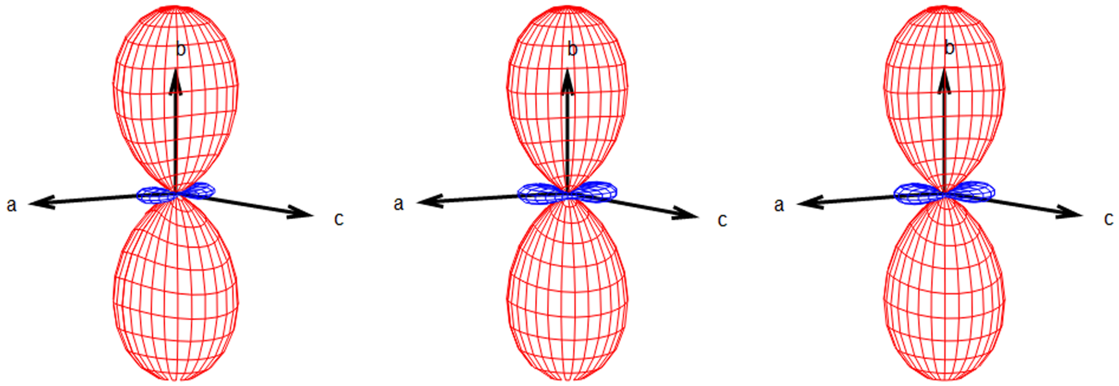

Figure S1 The expansivity indicatrix of **A** (100-340 K) (left), **B** (100-340 K) (middle), **B** (100-500 K) (right) relating the principal axes of thermal expansion (red = positive; blue = negative thermal expansion).[5]

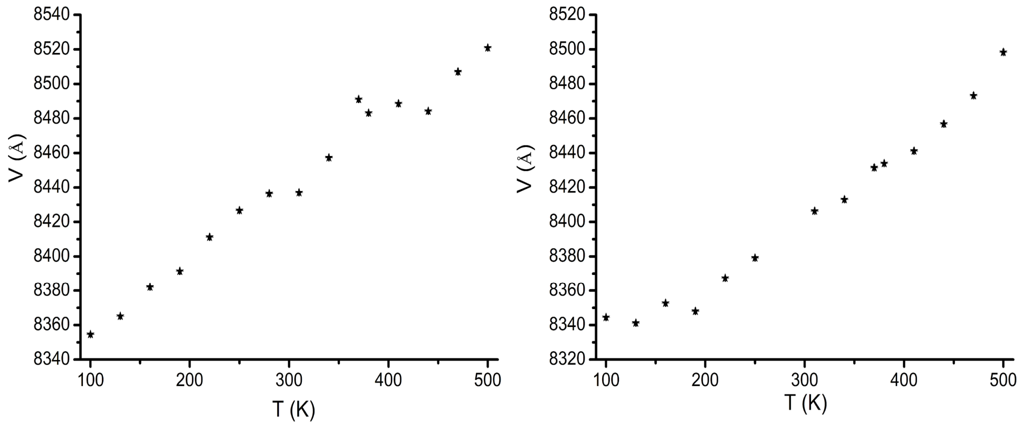

Figure S2 Unit cell volume of **A** (left) (**A** has converted to the dehydrated phase **B** at 370 K) and **B** (right) as a function of temperature.

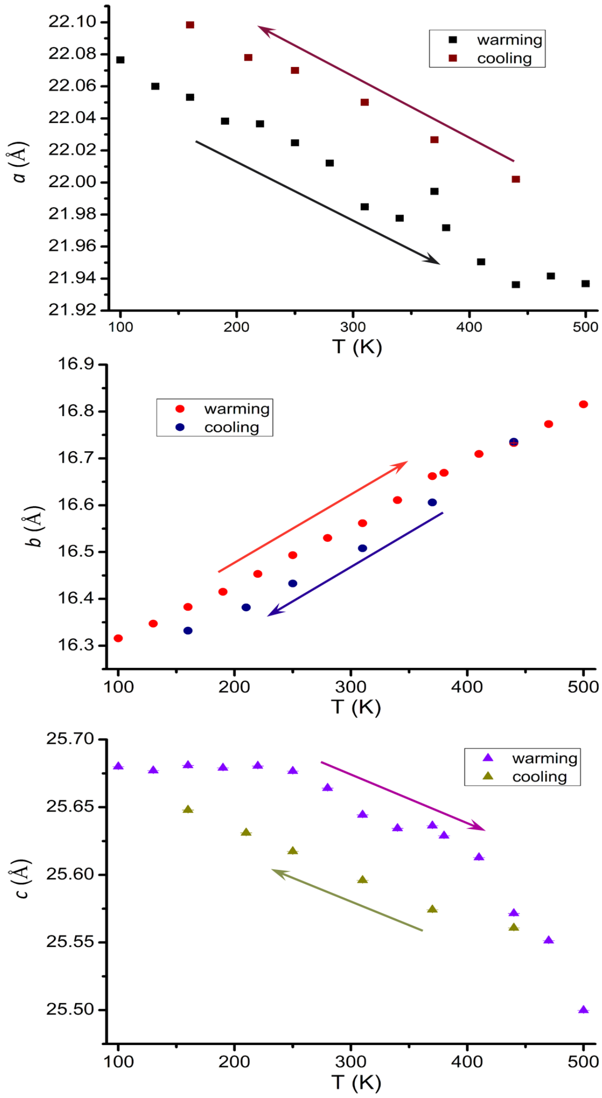

Figure S3 Temperature dependence of the *a*-, *b*-, and *c*-axis lengths of **A** warming from 100 K to 500 K and cooling from 500 K to 160 K (**A**

has converted to the dehydrated phase **B** at 370 K, and its cooling form as **A’** that is **B**).

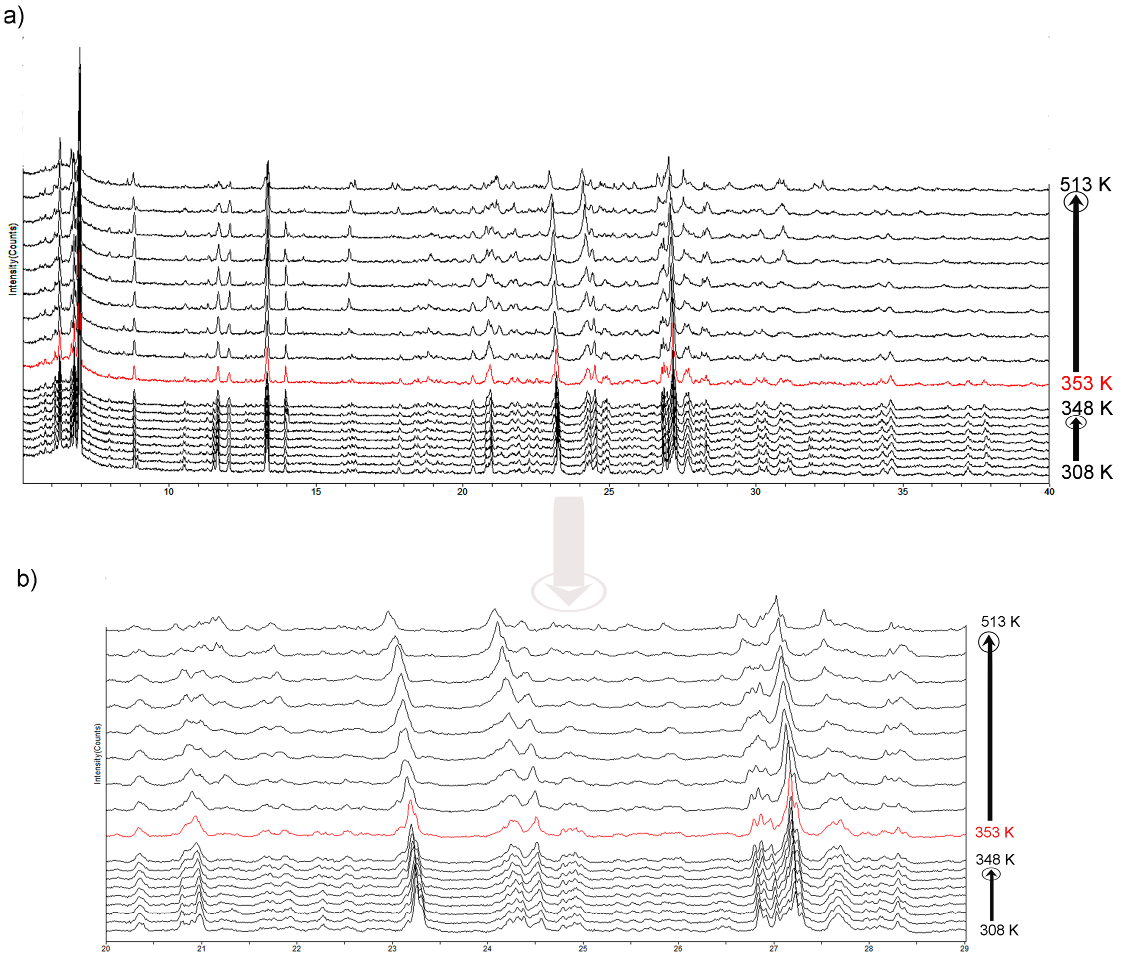

Figure S4 Uncorrected VT-PXRD patterns of **A** recorded from 308 K to 348 K with a step size of 5 K, then from 353 K to 513 K (△T/step = 20 K) (**A** has converted to the dehydrated phase **B** at 353 K). b) is part of a).

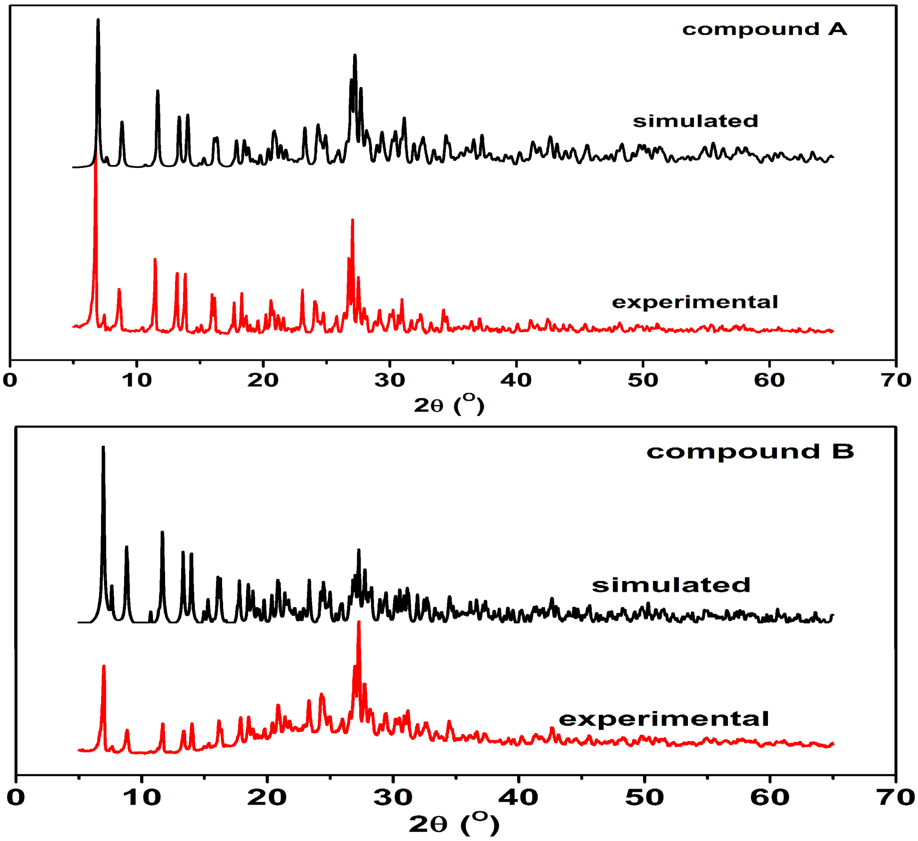

Figure S5 PXRD of compound **A** and its corresponding dehydrated phase **B** at room temperature. The phase purity for **A** and **B** was examined. Calculated pattern from the single crystal structure of **A** and **B** (black); observed from an as-synthesized sample of **A** and **B** (red).

Physical Measurement

Thermal Analysis-Quadrupole Mass Spectrometer

Thermogravimetric analysis (TGA) and Mass spectrometer (MS) show that **A** can be stable up to 300 °C, meanwhile, there is discrete guest water molecules located in the crystalline lattice of **A** as water molecules peak on the MS curve at 71 °C (Figure S4a, S4b), however, the samples that are heat treated at 100 and 220 ºC respectively prior to the MS measurements show that have no peeks of the molecule weigh 17 and 18 from Mass Spectrometer. With regard to Mass Spectrometer of the detected gas, the peaks of the molecule weigh 17 and 18 can be ascribe to H_2O molecule, the peak of the molecule weigh 28 may be attribute to the N_2 or CO gas molecules, the peaks of the molecular weight of 22 and 44 may be CO_2 molecule, and the peak of the molecule weigh 46 may be from NO_2 molecule.

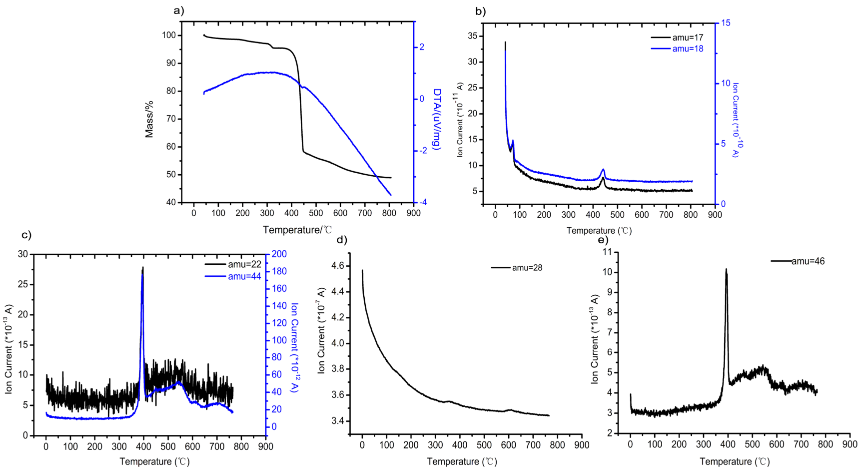

Figure S6 a) TG and DTA curve of **A** at room temperature. b), c), d), e) The Mass Spectrometer of the detected gas.

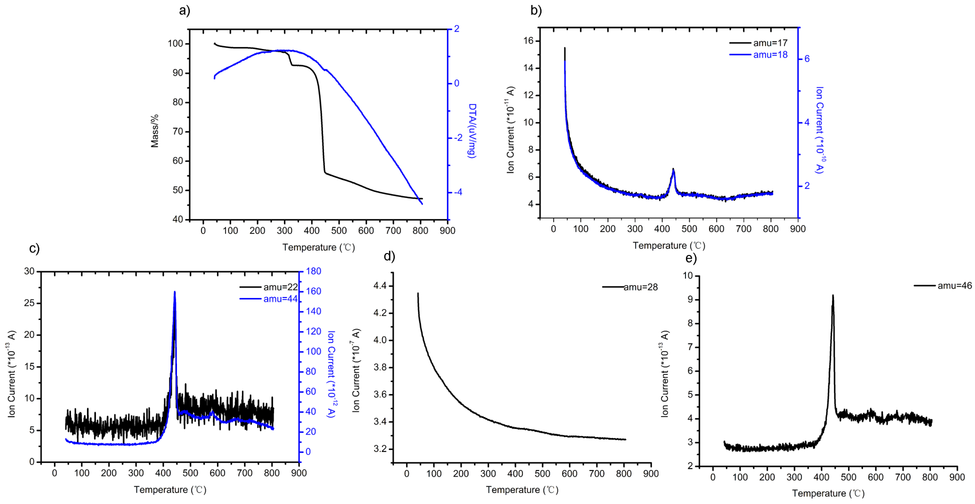

Figure S7 a) TG and DTA curve of **A** that is heat treated at 100 ℃ (**A** has converted to the dehydrated phase **B**). b), c), d), e) The Mass Spectrometer of the detected gas.

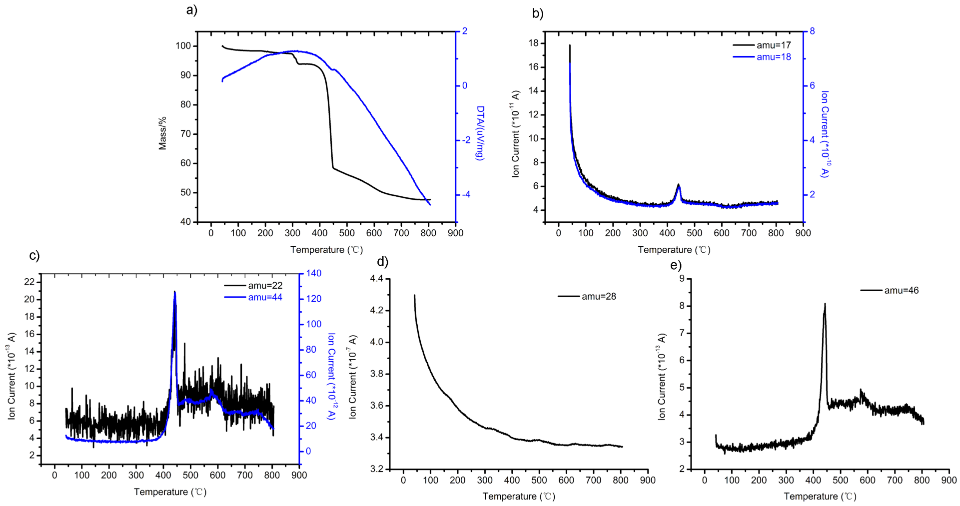

Figure S8 a) TG and DTA curve of **A** that is heat treated at 220 ℃ (**A** has converted to the dehydrated phase **B**). b), c), d), e) The Mass Spectrometer of the detected gas.

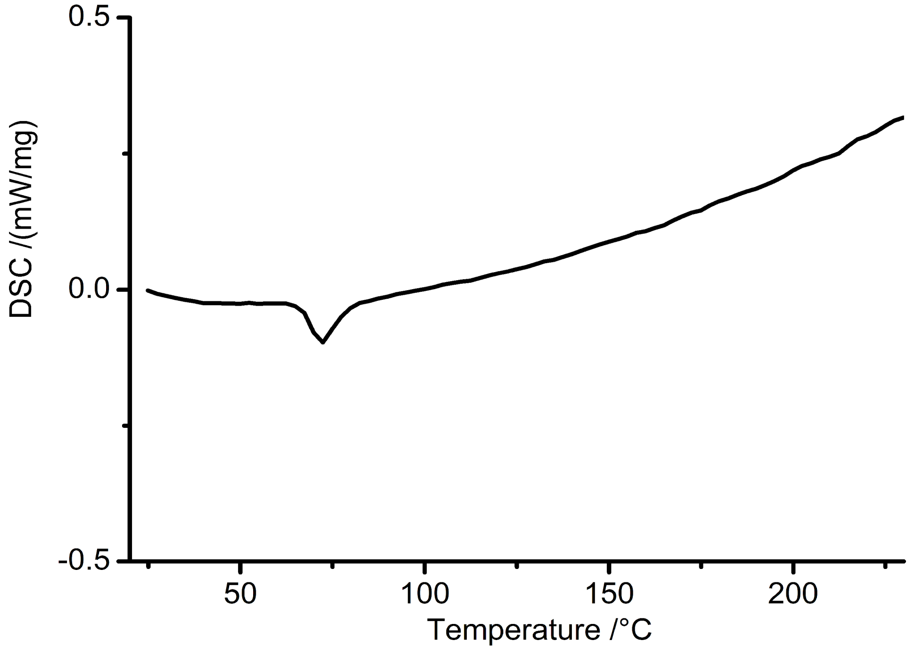

Figure S9 DSC of **A** measured in the range from 25 to 230 ºC under a nitrogen atmosphere with a heating rate of 5 ºC per minute. At 62 ºC, **A** starts to lose guest water molecules accompanied with the heat release behavior.

Additional Figures and Descriptions

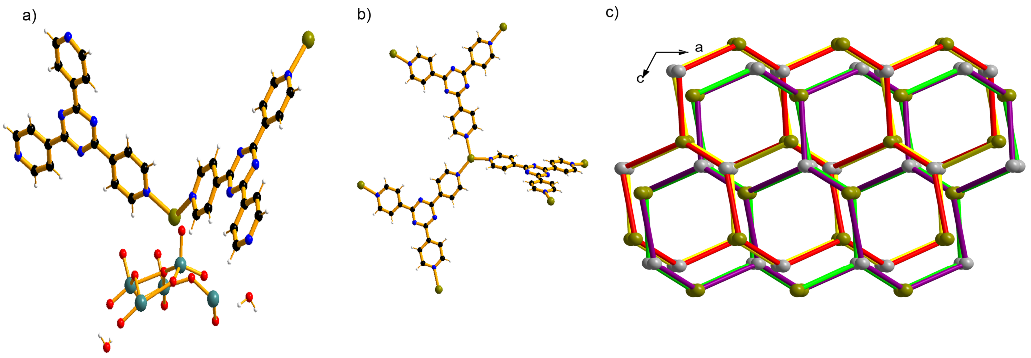

Figure S10 a) The asymmetric unit of **A** at 100 K. b) The coordination environment of Ag(**I**) atom and tpt in **A** at 100 K. c) The interpenetration of the four 10^3-**ths** nets comprised within **A**.

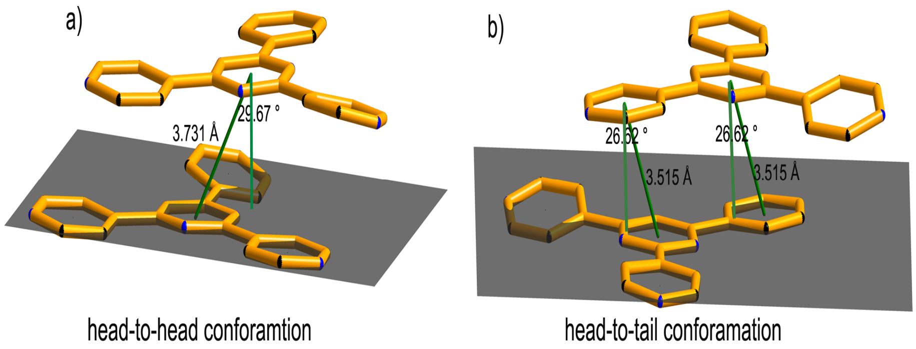

Figure S11 a) The centroid–centroid distances of head-to-head conformation (□ and □, □ and □) and the twisted angle of **A** at 100 K; b) The centroid–centroid distances of head-to-tail conformation (□ and □, □ and □) and the twisted angle of **A** at 100 K.

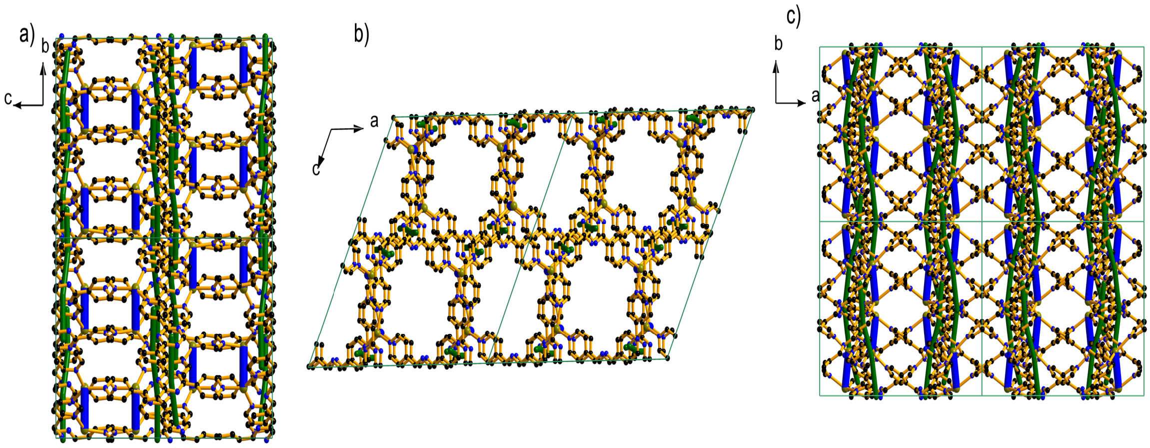

Figure S12 Schematic illustration showing the argentophilic and π-π interactions in the host framework of **A** and **B**, viewed along the *a*-axis (left), along the *b*-axis (middle), and along the *c*-axis (right). The olive lines depict π-π interactions and the blue lines represent Ag···Ag interactions.

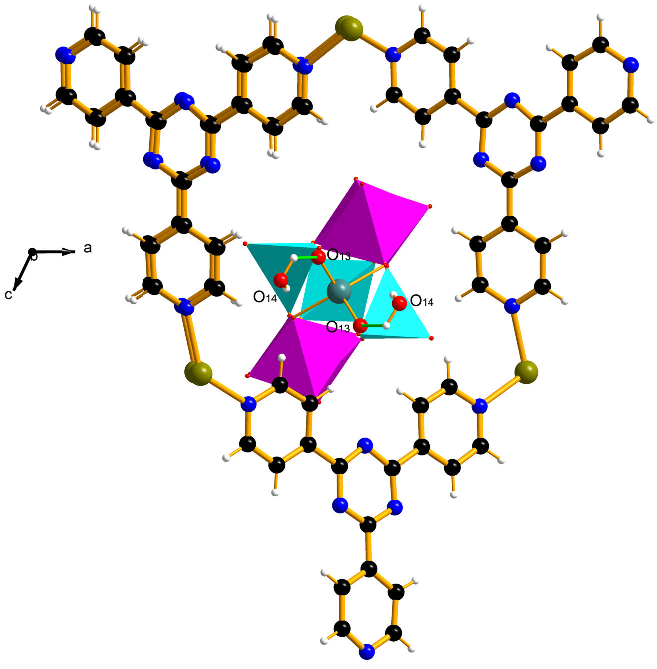

Figure S13 Schematic illustration showing the hydrogen bond interaction of O_{13} (the terminal oxygen atoms of δ-$[Mo_8O_{26}]^{4-}$) and O_{14} (H_2O) in **A**. The green lines depict O-H···O contacts.

References

[1] M. X. Li, Z. X. Miao, M. Shao, S. W. Liang and S. R. Zhu, *Inorg. Chem.*, **2008**, *47*, 4481-4489.

[2] a) P. K. Allan, B. Xiao, S. J. Teat, J. W. Knight and R. R. Morris, *J. Am. Chem. Soc.*, **2010**, 132, 3605-3611; b) I. Grobler, V. J. Smith, P. M. Bhatt, S. A. Herbert and L. J. Barbour, *J. Am. Chem. Soc.*, **2013**, 135, 6411-6414.

[3] J. Cosier and A. M. Glazer, *J. Appl. Crystallogr.*, **1986**, 19, 105–107.

[4] G. M. Sheldrick, *Acta. Crystallogr.*, **2008**, A64, 112-122.

[5] M. J. Cliffe and A. L. Goodwin, *J. Appl. Cryst.*, **2012**, 45, 1321-1329.